

Preparation and Characterization of Microwave sintered SrFe₁₂O₁₉/NiFe₂O₄ nanocomposite

Dissertation submitted in fulfillment of the requirement for the Degree of

MASTER OF SCIENCE

BY

Ishita Sharma

(301704014)



THAPAR INSTITUTE
OF ENGINEERING & TECHNOLOGY
(Deemed to be University)

Under the supervision of

Dr. PUNEET SHARMA

(Associate Professor)

School of Physics & Material Science

THAPAR INSTITUTE OF ENGINEERING AND TECHNOLOGY

PATIALA (147004)

PUNJAB

JULY-2019

CERTIFICATE

I hereby certify that the work which is being presented in the report entitled "**Preparation and Characterization of Microwave sintered SrFe₁₂O₁₉/NiFe₂O₄ nanocomposite**" submitted by me in partial fulfillment of the requirement for the degree of **M.Sc. Physics** is an authentic record of my own work carried under the supervision of **Dr. Puneet Sharma**, School of Physics and Material Science at Thapar Institute of Engineering and Technology, Patiala (147004).


The matter presented in this thesis has not been submitted by me for the award of any degree of this or any other university.


15/7/2019
Ishita Sharma

(301704014)

This is to certify that the above mentioned statement of the student is correct to the best of my knowledge and belief.

Date: 13th July, 2019


Dr. Puneet Sharma
Associate Professor
School of Physics and Material Science
Thapar University, Patiala (147004)

ACKNOWLEDGEMENT

Foremost, I would like to express my sincere gratitude to **Dr. Puneet Sharma**, Associate Professor (SPMS), for giving me an opportunity to work under his supervision, without whose help and constant guidance this thesis would have not taken place. I am extremely thankful to **Prof. O. P. Pandey**, Head (SPMS) for their co-operation and encouragement. I am also thankful to all the members of SPMS for their constant co-operation during experimental work.

I am highly thankful to **Chhavi Pahwa, Santhosh Kumar Mahadevan, Shivani Jindal, Anoop Partap Singh and Parminder Singh**, research scholars SPMS, who provided their valuable guidance and suggestions during the work. I acknowledge and thank my elders, my friends and my fellow classmates for their support and constant motivation. Last but not least, I am very thankful to my parents for their constant support, patience and blessings.

Table of Contents

Acknowledgement	ii
Table of contents	iii
List of figures	iv
List of Tables	v
List of Flowcharts	v
Abstract	vi
Chapter-1 Introduction	1-9
1.1 Ferrites	2
1.2 Soft Ferrites	3
1.3 Hard Ferrites	4
1.4 Composite ferrite	5
1.5 Synthesis methods for ferrites	7
1.6 Application of Ferrites	8
1.7 Motivation	8
1.8 Objectives	9
Chapter-2 Literature review	10-20
2.1 Spinel ferrite	11
2.2 Hexaferrites	14
2.3 Ferrite Composite.....	17
Chapter-3 Experimental details	21- 27
3.1 Synthesis of Soft ferrite (NiFe_2O_4) powder	22
3.2 Synthesis of Hexaferrite ($\text{SrFe}_{12}\text{O}_{19}$) powder	24
3.3 Synthesis of SrM/NiF composite	25
3.4 Characterization technique	27
Chapter-4 Results and discussion	28-38

Conclusion.....	39
References	40-48

List of Figures

Figure 1.1 Classification of Ferrites	2
Figure 1.2 Spinel crystal structure	4
Figure 1.3 Unit cell of $\text{SrFe}_{12}\text{O}_{19}$	5
Figure 1.4 Composite ferrite	6
Figure 3.1 Dendritic ash flakes of ferrite	23
Figure 3.2 Rotatory Ball mill and Zirconia jar with balls	25
Figure 3.3 Microwave furnace	26
Figure 4.1 XRD pattern of pure NiF, SrM and SrM/NiF (70/30) nanocomposite	29
Figure 4.2 XRD patterns of microwave sintered SrM and SrM/NiF (50/50) nanocomposite	31
Figure 4.3 <i>M-H</i> loops of (a) SrM & NiF, and (b) physically mixed SrM/NiF nanocomposite powders.....	32
Figure 4.4 Variation in theoretical and experimental observed (a) M_s and (b) H_c of SrM/NiF nanocomposite with NiF content	34
Figure 4.5 <i>M-H</i> loop of sintered (a) SrM and NiF (b) SrM/NiF nanocomposite with different composition (c) powder and sintered 70/30 composite	35
Figure 4.6 Variation in theoretical and experimental observed (a) M_s and (b) H_c of SrM/NiF nanocomposite with NiF content sintered at 1200 °C	37
Figure 4.7 SEM micrographs of (a) NiF (b) SrM and (c) SrM/NiF (70/30)	

sintered at 1200 °C.....38

List of Tables

Table 1.1 Classification of Spinel ferrites	3
Table 1.2 Classification of Composite ferrites	6
Table 1.3 Magnetic Properties of ferrite	9
Table 4.1 Crystallite size of SrM and NiF for pure and composite powder	30

List of Flowcharts

3.1 Flow chart for synthesis of Nickel Ferrite (NiFe_2O_4) by sol-gel auto combustion	23
3.2 Flow chart for synthesis of Strontium ferrite ($\text{SrFe}_{12}\text{O}_{19}$) by sol-gel auto combustion method	24
3.3 Flow chart for synthesis of SrM/ NiF composite by physical mixing method	26

ABSTRACT

In the present work, microwave sintered nanocomposite of NiFe_2O_4 (NiF) and $\text{SrFe}_{12}\text{O}_{19}$ (SrM) in different weight fraction (80/20, 70/30, 60/40, 50/50) were prepared. Their phase, microstructure and magnetic properties were analyzed by X-ray diffraction (XRD), Scanning Electron Microscope (SEM) and Vibrating Sample Magnetometer (VSM) respectively. X-ray diffraction pattern confirmed co-existence of both spinel (NiFe_2O_4) and hexagonal ($\text{SrFe}_{12}\text{O}_{19}$) phases in sintered composites without any secondary phase. Kinked demagnetization curve was observed for powders as well as sintered composites. However kink was more prominent in powder samples. Obtained kink in $M-H$ loops indicating non-exchange coupling between hard/soft phases. Contrary to powders, microwave sintered composites showed higher M_s values from theoretical calculated one confirmed that sintering adequately enhance the coupling between hard/soft phases.

Chapter 1

Introduction

Overview

In this chapter, basic description of ferrites and their crystal structures are given. Classification of ferrites based upon magnetic and structural properties has been described. Further, different synthesis routes and applications of ferrites are summarized. In the end, motivation and objectives of the thesis are given.

1.1 Ferrites

Ferrites are ceramic compounds of iron oxide (Fe_2O_3) mixed with one or more metallic ions. The general chemical formula of ferrite is $\text{A}(\text{Fe}_x\text{O}_y)$ where A represents divalent metallic ion such as Cu, Fe, Zn, Ni, Co, Mg, Ba or Mn [1]. The crystal structure of ferrite consisted of closed packed, oxygen ions where cations occupy interstitial sites. Ferrites are ferrimagnetic in nature as the magnetic moment of their constituent atoms are aligned in different direction which results in partial cancellation of magnetic moment [2]. Ferrites magnets are generally used for devices such as refrigerator, loud speaker, inductor and transformer cores etc [1-3]. Nanocrystalline ferrites have fascinating applications in electronic, telecommunication and microwave components. Low eddy current and dielectric loss makes ferrites preferential over other materials for microwave application purpose [4]. Generally, ferrites are distributed in four main categories including spinel, garnet ferrites (cubical structural arrangement), hexaferrites (hexagonal arrangement) and orthoferrite (perovskite) [5].

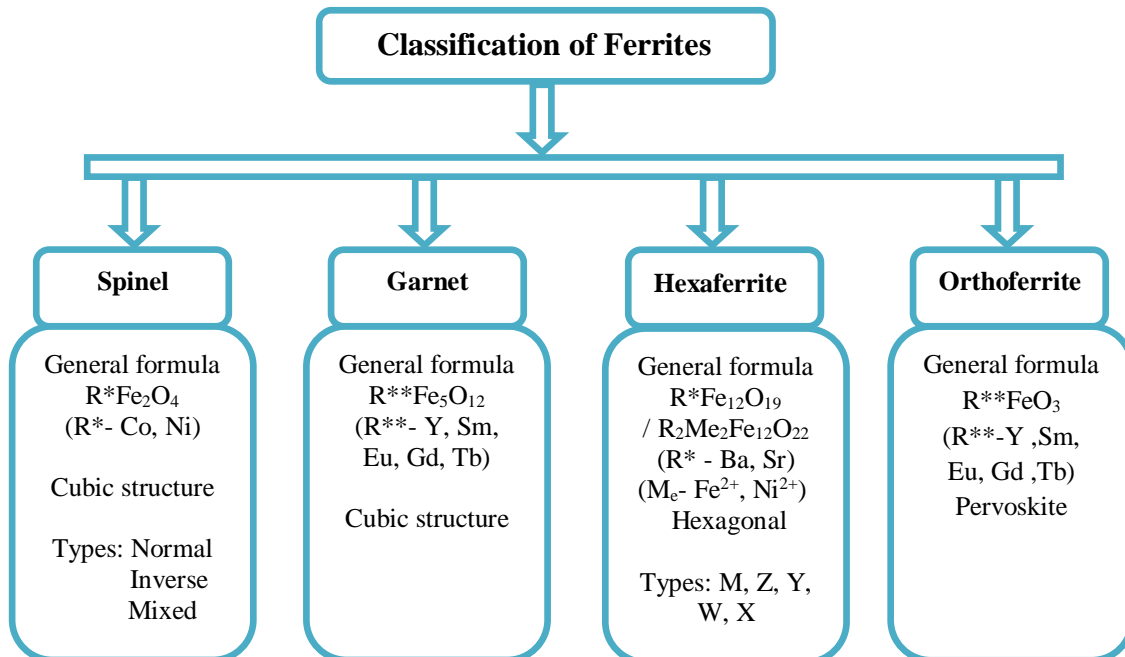


Fig. 1.1 Classification of Ferrites

On the basis of their magnetic characteristics, ferrites are distinguished as

- ❖ Soft ferrites
- ❖ Hard ferrites.

1.2 Soft ferrites

Materials which can be magnetized and demagnetized easily with applied field are termed as soft ferrites. The general chemical formula for soft ferrite is $M^*Fe_2O_4$ (M^* represents any rare or transition metal ion) [6]. Soft ferrites are important branch of ferrites because of their high saturation magnetization (M_s), electrical resistivity, low coercivity (H_c), low anisotropy (H_a) and low dielectric losses [7,8]. They also have low eddy current, low magnetostriction and high permeability. Energy dissipation is very less as magnetic dipoles easily reverse the direction due to its low coercivity. Soft ferrites have spinel configuration which comprises of 32 closed packed oxygen ions forming tetrahedral (64) and octahedral (32) interstitial sites [8]. On the basis of distribution of divalent metallic ions on respective tetrahedral and octahedral sites, spinel ferrites are classified as **Normal**, **Inverse** and **Mixed spinel**.

Table 1.1 Classification of Spinel ferrites

Spinel	Tetrahedral site (A)	Octahedral site (B)
Normal	All divalent (Ni^{2+} , Co^{2+} , Cu^{2+} , Zn^{2+}) metallic ions	All trivalent (Fe^{3+}) metallic ions
Inverse	Half trivalent ions	Divalent and half trivalent ions
Mixed	Both divalent and trivalent ions	Both divalent and trivalent ions

In the present work, we used NiFe_2O_4 as soft phase which exhibits inverse spinel geometry and unit cell of NiFe_2O_4 is shown in fig. 1.2.

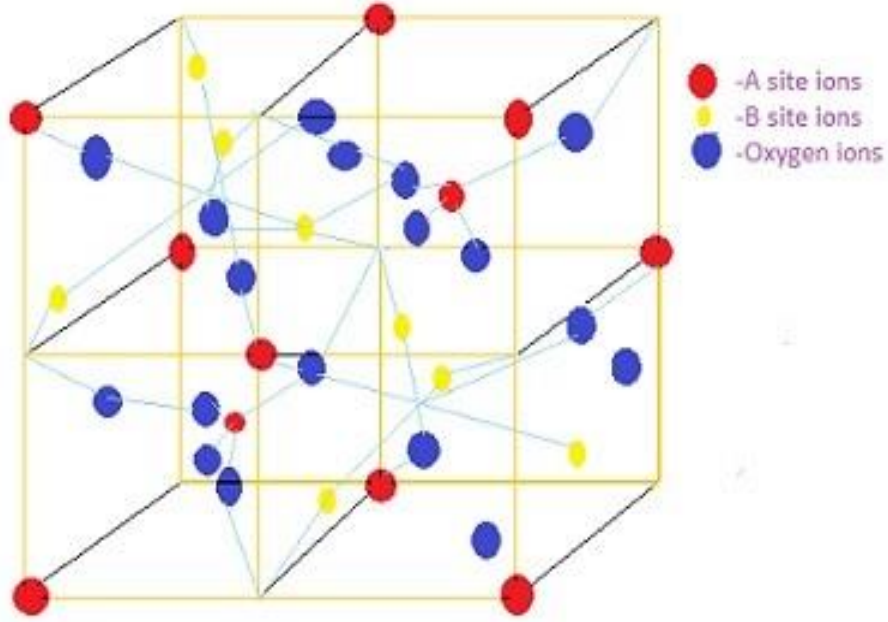


Fig. 1.2 Spinel crystal structure

1.3 Hard ferrites

Materials which cannot be easily magnetized and demagnetized with applied field are termed as hard ferrites. The general chemical formula for M-type ferrite is $\text{M}^*\text{Fe}_{12}\text{O}_{19}$ ($\text{M}^* = \text{Ba}^{2+}, \text{Sr}^{2+}, \text{Pb}^{2+}$). Hard ferrites exhibit not only high coercivity (H_c) but also high resistivity, Curie temperature (T_c), remanent magnetization (M_r) and anisotropy (H_a) [9, 10]. These remarkable properties of hexaferrites have made them one of the most investigated magnetic materials for permanent storage application. These ferrites generally exhibit magnetoplumbite structure [11].

In the present work, $\text{SrFe}_{12}\text{O}_{19}$ is used as hard phase. A molecular unit of $\text{SrFe}_{12}\text{O}_{19}$ comprises of mainly two blocks: block S (spinel type structure) and block R (hexagonal structure) in which oxygen ions are

arranged in closed-packed layers. Fe^{3+} ions are distributed among five distinct crystallographic sites namely 12k, 4f₂, 2a (octahedral), 4f₁ (tetrahedral) and 2b (trigonal bi-pyramidal). Among these different crystallographic sites 12k, 2a and 2b have up spin while 4f₂, 4f₁ have down spin [9,11].

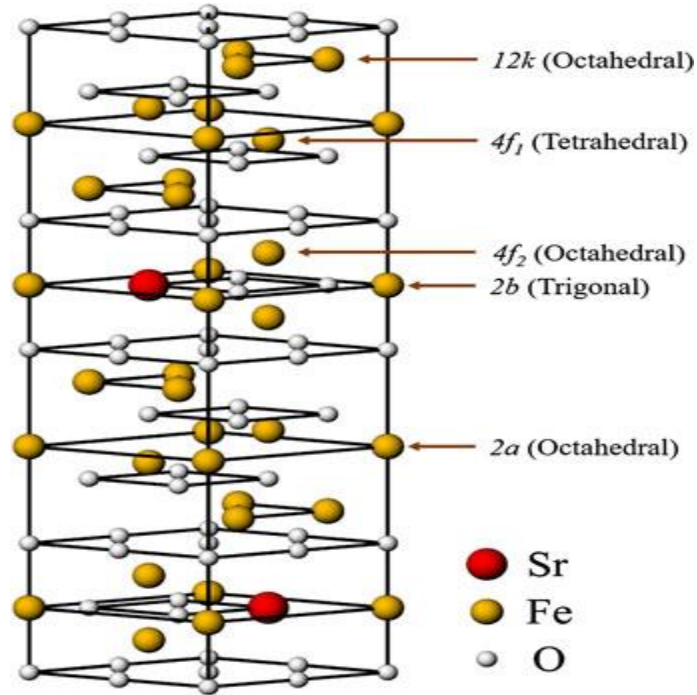


Fig. 1.3 Unit cell of $\text{SrFe}_{12}\text{O}_{19}$ [12]

1.4 Composite ferrite

Apart from hexaferrites and spinel ferrites, the composites of high anisotropy (H_a) hard phase and high M_s soft magnetic phase has gained considerable attention for microwave application and high energy product magnets. The concept of composite system was first given by Kneller and Hawig in 1990s to improve magnetic properties of the material. The studies on such system were broadly divided into two classes: alloy based composite and oxide based composite (Table 1.2) [13].

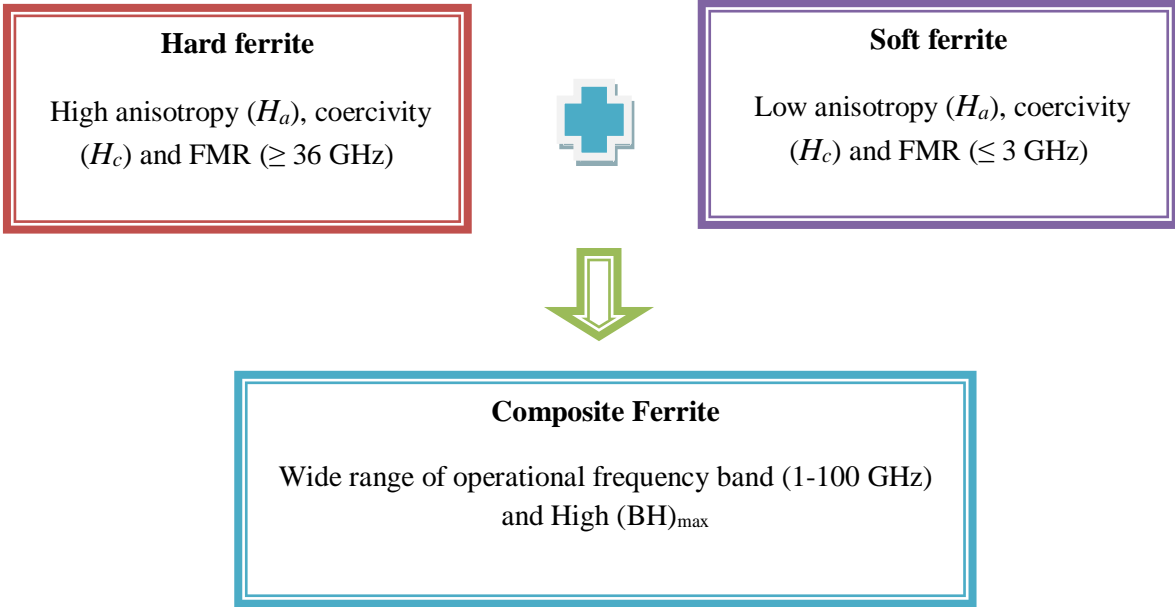


Fig. 1.4 Composite ferrites

Table 1.2 Classification of composite ferrites

Composite	Example
Alloy based composite	Fe-Ni, Fe-Pt, Nd-Fe-B, Sm-Co/Fe [14,15]
Oxide based composite	SrFe ₁₂ O ₁₉ /γ Fe ₂ O ₃ , (Mn,Zn) Fe ₂ O ₄ /CoFe ₂ O ₄ , Ni _{0.8} Zn _{0.2} Fe ₂ O ₄ /BaFe ₁₂ O ₁₉ [16,17]

Alloy based composites and bilayer thin film system has gained attention in high energy product magnets, while oxide based composite systems for microwave absorbing materials [18]. However, in such system interfacial exchange interaction are responsible for enhancement of $(BH)_{\max}$ and measured by demagnetization curve of the $M-H$ loop. If two phases are strongly coupled; a smooth hysteresis curve obtained which corresponds to coherent rotation of spins at the hard-soft interface. Whereas,

stepped $M-H$ loop signifies uncoupled system i.e. couplings among two phases is non-coherent at the interface. Demagnetization curves with and without kink for the composite systems were referred as non-exchange and exchange coupled systems respectively. In case of nanoparticles, coupling strongly depends upon distribution of particle size while for thin films; thickness of film decides the extent of coupling [18]. Coupling phenomenon is highly sensitive towards various parameters such as synthesis process and annealing temperature [19]. As composite ferrites are the mixture of high FMR hard phase and low FMR soft phase, hence could be a possible material for high frequency device application operable in wide frequency band.

In present work, $\text{SrFe}_{12}\text{O}_{19}$ and NiFe_2O_4 were physically mixed and their respective magnetic, structural and surface morphological properties were investigated.

1.5 Synthesis methods for ferrites

Different processing methods are used for synthesis of ferrites as electrical and magnetic properties of ferrites are highly sensitive towards synthesis process. Some of the highly preferable methods are listed below [5].

- Sol gel auto combustion
- Hydrothermal method
- Chemical co-precipitation
- Solid state synthesis

In the present work, soft ferrite (NiFe_2O_4) and hard ferrite ($\text{SrFe}_{12}\text{O}_{19}$) were prepared by sol-gel auto combustion route. Synthesis mechanism is explained in experimental section.

1.6 Application of Ferrites

Ferrites have numerous applications due to their phenomenal magnetic and microwave properties. Ferrites are used in multilayered chip inductor, transformer core, gas sensors, recording media, antennas, frequency devices, computers, radios [20]. Due to low coercivity (H_c), high electrical resistivity, permeability (μ) and low eddy current losses; soft ferrites have tremendous applications in AC/DC convertors, fabrication of radio frequency coils, rod antennas, resistive switching, transformer cores, ferro-fluids, electromagnetic noise suppressors, RF inductors, hyperthermia as well as chemical sensors [21, 22]. Characteristic properties of hexaferrites such as high resistivity, high Curie temperature, high anisotropy made them favorable for various applications such as permanent magnets, microwave antennas, isolators, wireless communication, magnetic recording media, phase shifters, loud speakers, microphones [9, 10]. Composites are used in biomedical applications, electromagnetic wave absorbers and magnetic recording media [18]. Composite ferrites are also used in superior permanent magnets due to high energy product (BH_{\max}) [19].

1.7 Motivation

With the development of technology, modern microwave ferrite includes spinel, garnet and hexagonal has gained attention in microwave industry due to their characteristic electrical and magnetic properties. However, low anisotropic spinel ferrites with low FMR limits their application to the MHz range whereas hexaferrite with high FMR works in GHz range (Table 1.3). Hence, recently focused has been laid on the composite ferrite comprises of high anisotropic hard phase and high M_s soft phase as they can be used in the wide frequency band (1-100 GHz). The effect of processing of such composites plays a dominant role, which leads to exchange coupled and non exchanged coupled behavior of composites. Various studies reported that composites processed by physical mixing of individual powders showed

non-exchange coupled behavior, whereas single step method showed high coupling. Further, the sintering of such composites also affects the coupling. Till now, exchange coupling in conventionally sintered magnets has been investigated. No reports are available on microwave sintered hard/soft composites. In the present work, microwave sintered composites of SrFe₁₂O₁₉ /NiFe₂O₄ in the weight ratios of 80/20, 70/30, 60/40, 50/50 were prepared and their structural and magnetic properties were investigated.

Table 1.3 Magnetic Properties of ferrites

Material	T_N (°C)	4πM_s (Gauss)	Coercive field H_c (Oe)	Magnetic anisotropy H_a (Oe)
SrFe₁₂O₁₉	455 [23]	4320 [25]	6635 [24]	16,000 [23]
NiFe₂O₄	585	3000	5.7	425

1.8 Objectives

1. To Prepare SrFe₁₂O₁₉ /NiFe₂O₄ microwave sintered composite of various weight fraction.
2. To investigate structural and magnetic properties of microwave sintered composites.

Chapter 2

Literature Review

Overview

Large amount of research has been carried out to investigate magnetic and structural properties of ferrites. This section briefly addresses the important work done in last few years on spinel, hexagonal and composite ferrites.

2.1 Spinel ferrite

Spinel ferrites have gained much importance in last five decades and were first successfully examined in 1945 by J.L. Snoek. Their vast applications including inductor coil, biosensors, electronic media, MRI agents were matter of great attention in these years. In this section we have summarized the work done in recent years to investigate magnetic and microwave absorption properties of spinel ferrites and effect of parameters such as substitution concentration, synthesis route, heating medium on these properties.

In 1996, M.A. El Hiti et al. [26] prepared series of Ni-Mg ferrite with Zn substitution using usual ceramic method. They found that with increase in temperature electric parameters such as real dielectric constant, ac conductivity and dielectric loss tangent increases. While activation energy, dielectric constant and dielectric losses were found to decrease with the frequency. They also observed shifts in relaxation frequency f_D towards higher values with increase in temperature. The results suggested that both electric and dielectric parameters were found to depend upon composition and temperature. **In further year 2005, Anjali Verma et al. [27]** used citrate precursor method to synthesize $Ni_{1-x}Zn_xFe_2O_4$ ($x = 0.2, 0.4, 0.5$ and 0.6). Dielectric measurements were performed at X-band (8 - 12 GHz) and observed dielectric constant values lies in range 5.5 - 7.9 for particles sintered at 1200 °C. Whereas for particles sintered at 1300 °C, higher dielectric constant (9-10) were observed as compared to particles sintered at 1200 °C. Results showed that permittivity losses were of order 10^{-2} - 10^{-3} . DC-resistivity of the samples lies between 10^7 - 10^{11} Ω cm. The different sintering temperature strongly effect the grain size growth and responsible for resultant high resistivity and low dielectric losses. These results suggested that $Ni_{1-x}Zn_xFe_2O_4$ nanoparticles are suitable for high frequency practical applications.

In 2006, C. P. L. Rubinger et al. [28] synthesized nanocrystalline $NiFe_2O_4$ by micelles mixing technique and used lyophilized coconut oil. Change in crystallite size with annealing temperature (400,

600, 800, 1000, 1200 °C) was investigated by X-ray diffraction (XRD) analysis. They performed complex permittivity measurements in cavity resonators at 5 and 9 GHz and real part of permittivity was found to decrease (3.6 - 2.4) with temperatures whereas the imaginary part showed variation only at low temperature. **Further, in 2008 John Jacob et al. [1]** used another method namely chemical co-precipitation route for synthesis of nanocrystalline nickel ferrite particles. They investigated the dielectric properties in frequency range 2.4 - 4 GHz and determined the values of dielectric constant, microwave heating coefficient and dielectric loss. They concluded that there is substantial change in values of dielectric constant, heating coefficient as well as dielectric loss with average grain size.

In 2009, M. Sertkol et al. [29] synthesized $Zn_xNi_{1-x}Fe_2O_4$ nanoparticles using combustion method (urea as fuel) assisted by microwave sintering. The average crystallite size of Ni-Zn particles was ~20nm and particles showed spherical symmetry as confirmed by SEM analysis. Dependence of magnetic properties on ions (Ni, Fe and Zn) positions was also investigated. Highest value of $M_s \sim 41.89$ emu/g was observed for $x = 0.2$. **In consecutive year, Xue gang et al. [30]** prepared Ni-Zn nanoparticles via co-precipitation method and investigated its structural as well as magnetic properties. Saturation magnetization of Ni-Zn particles was 60 emu/g. In dielectric results; a broad peak of imaginary permeability (μ'') in frequency range 200 MHz to 6 GHz was observed which corresponds to the magnetic losses of the materials. These results recommend that Ni-Zn ferrites can be used in high frequency electromagnetic absorption applications.

In 2013, Stevan M. Ognjanovic et al. [31] prepared $NiFe_{2-x}Y_xO_4$ via co-precipitation method (where $0 \leq x \leq 0.3$). X-ray diffraction pattern confirmed the formation of secondary phases for $x > 0.07$. With addition of Y^{3+} ion, the grain size was found to decrease. Dielectric measurements were carried out in frequency range 100 Hz-1MHz. AC conductivity found to increase while $\tan\delta$ decrease with addition of

Y^{3+} ion. High ac conductivity and small $\tan\delta$ values make the material suitable for microwave applications.

In the next year, M. Penchal Reddy et al. [32] prepared $NiFe_2O_4$ nanoparticles followed by microwave sintering. Single ferrite phase and crystallite size of the order of 30nm was confirmed by X-ray diffraction pattern. Microwave sintered sample showed high saturation magnetization (M_s) ~ 55.27 emu/g as compared to conventionally sintered sample. Results suggest that magnetic properties can further be modified not only by substitution but also by effective sintering environment. **In 2015, Ch. Srinivas et al. [33]** prepared series of $Ni_xZn_{1-x}Fe_2O_4$ where $x = 0.5, 0.6$ and 0.7 via coprecipitation technique to study structural as well as magnetic behavior of the sample. Increase in crystallite size with Ni substitution was observed which corresponds to decrease in strain. At room temperature, nanoparticles showed super paramagnetic behavior. An increase in hyperfine interaction in nanoparticles was observed which further cause decrease in core-shell interaction with Ni^{2+} ion concentration substitution. **In the consecutive year, S.Prasath et al. [34]** prepared $Ni_{1-x}Zn_xFe_2O_4$ where $x = 0, 0.2$ and 0.4 and investigated its suitability for microwave (L band) antenna applications. XRD analysis confirmed the transformation of inverse spinel structure to normal spinel structure with the addition of Zinc. A drastic increase in resonance value was observed with Zn substitution. Real part of permeability was found to be constant at 2.0 in L band frequencies (1 - 2.0 GHz) for $x = 0.2$. A shift in resonance frequency at lower side suggests that these materials can be used as miniaturized patch antenna. **In the same year, G. Umopathy et al. [35]** used combustion method to prepare $Ni_{1-x}Zn_xFe_2O_4$ [$x = 0.0, 0.25, 0.50, 0.75, 1.0$]. Lattice parameter was found to be increase from 8.348 to 8.443 Å with increase in Zn^{2+} ion concentration. Dielectric measurements were performed and a decrease in dielectric parameters was observed. Impedance measurements showed change in size, grain boundaries and resistance of material.

2.2 Hexaferrites

Among the family of hexagonal ferrites, Barium and Strontium ferrites have gained significant attention in last few decades because of their unique characteristic properties such as high magneto anisotropy, coercivity, moderate saturation magnetization along with high FMR frequency. This literature survey focuses at magnetic and microwave properties of pure and substituted hexaferrite for modern microwave device applications.

In early 90s, R. Muller et al. [36] prepared Co-Ti substituted $\text{BaFe}_{12-2x}\text{Co}_x\text{Ti}_x\text{O}_{19}$ using glass crystallization method and annealed the sample for different temperatures ranging 300-1200 °C. Average particle size increases with temperature. Magnetic measurements were performed and decrease in H_c , M_r was reported. **Further, H. Pfeiffer et al. [37]** prepared $\text{BaFe}_{12-2x}\text{Co}_x\text{Ti}_{x-y}\text{Sn}_y\text{O}_{19}$ by same method and studied the effect of substitution on geometric and magnetic properties. Geometric measurements were performed and average diameter, aspect ratio showed decrease from 62.2 to 50.4 nm and 5.9 to 3.5 respectively. Decrease in magnetic parameters, H_c (1615 to 705 Oe) and H_r (1900 to 957 Oe) was reported. **C. Suring et al. [38]** used chemical route to synthesize pure and substituted (Co^{2+} , Zn^{2+}) BaM and SrM. For Co^{2+} substitution, anisotropy field at $x = 0.25, 5$ was found to be 1405 and 1180 kA/m. While Zn^{2+} substitution results in $H_A = 1090$ and 810 kA/m for $x = 0.25, 5$.

In 2010, Sachin Tyagi et al. [39] prepared $\text{SrFe}_{11.2}\text{Ni}_{0.8}\text{O}_{19}$ via co-precipitation technique. To study the effect of annealing temperature on magnetic parameters, powders were annealed at 900 °C and 1200 °C temperature in N_2 environment. Magnetic measurements showed drastic increase in saturation magnetization value from 43.35 to 65.188emu/g with temperature. SEM results showed that as-synthesized particles have spherical whereas heat treated samples shows hexagonal platelet structure. Also an increase in permittivity and permeability of $\text{SrFe}_{11.2}\text{Ni}_{0.8}\text{O}_{19}$ with temperature was observed.

Moreover, sample annealed at 1200 °C showed maximum reflection loss -24.92 dB at frequency 11.1 GHz and could be used for microwave device application.

Then in 2011, S. Kanagesan et al. [40] used sol-gel synthesis for formation of BaFe₁₂O₁₉ nanoparticles. To study the effect of sintering, powder was sintered in conventional and microwave medium. XRD results confirmed single hexagonal phase of BaFe₁₂O₁₉ for both mechanism. Average grain size was found to be 3.19 and 4.38 μm for conventionally, microwave sintered particles respectively. High coercivity was obtained in case of microwave as compared to conventionally sintered particles.

In the year 2016, Z. Mosleh et al. [41] prepared polycrystalline Ba_{1-x}Ce_xFe₁₂O₁₉ (x = 0.0 - 0.2) using sol-gel method. Single magnetoplumbite phase was confirmed via XRD results and the average particle size was found to decrease with substitution. Highest values of saturation magnetization, coercivity was found to be 53 emu/g and 5088 Oe respectively. Maximum reflection losses of the order of 16.74dB (at 10.3 GHz) and -20.47 dB (at 16.22 GHz.) were obtained for the higher substitution of Ce (x = 0.15, 0.2).

In year 2017, Qian Liu et al. [42] prepared Ba(ZnSn)_xFe_{12-2x}O₁₉ by traditional solid state method. Shrinkage in grain size and decrease in saturation magnetization from 57.62 to 45.57emu/g with substitution was obtained. Rapid decrease in magnetocrystalline anisotropy constant was observed till x=1. Squareness ratio for material was found to be 0.81. Zn-Sn substituted BaM showed promising features to be used in low frequency millimeter instruments namely isolators, circulators. **In the same year, Hossein Nikmanesh et al. [43]** prepared BaCu_xMg_xZr_{2x}Fe_{12-4x}O₁₉ (x = 0.0 - 0.5) using co-precipitation method. Drastic decrease in coercivity (4420.2 to 161.64 G) was observed. A shift in resonance frequency to lower value was obtained with the reflection loss of -20.4 dB for x = 0.5.

Moreover, permittivity and permeability were also found to change in the studied frequency range (2-18 GHz).

In 2018, Jianfeng Chen et al. [44] synthesized Co^{3+} substituted $\text{Sr}_{0.5}\text{Ba}_{0.5}\text{Fe}_{12-x}\text{Co}_x\text{O}_{19}$ ($x = 0, 0.2, 0.4, 0.6, 0.8, 1$) using conventional ceramic technique and sintered at $1150\text{ }^\circ\text{C}$. According to site preferences, Co^{3+} ions generally preferred $4f_2$ and $2b$ sites with low and high concentration respectively. Decrease in magnetocrystalline anisotropy coefficient (2.88×10^5 - $1.47 \times 10^5 \text{ J/m}^3$) and saturation magnetization (26.85×10^4 - $18.72 \times 10^4 \text{ A/m}$) was observed. Squareness showed sharp decrease from 73 to 27 %. **Same year, Hossein Nikmanesh et al. [10]** prepared $\text{BaCo}_x\text{Cu}_x\text{Zr}_{2x}\text{Fe}_{12-4x}\text{O}_{19}$ by auto combustion method ($x = 0.0$ to 0.5). Drastic decrease in coercivity was observed from 3540 to 396 Oe. Maximum reflection loss for material was found to be -27.4 dB at 5.35 GHz .

In 2019, Santhoshkumar Mahadevan et al. [45] synthesized $\text{BaFe}_{12}\text{O}_{19}$ and $\text{BaFe}_{11.5}\text{Ti}_{0.5}\text{O}_{19}$ using ball milling method and further calcined the sample three times at $1200\text{ }^\circ\text{C}$. FTIR and Raman confirmed the occupancy of Ti^{4+} ions in lattice site and a contraction in bond length with each calcination step. Microwave studies were performed by Vector Network Analysis in K_u -band (12.4 - 18 GHz). Results showed that, absorbance was higher in BaTiM than BaM and depends on the calcination conditions. **In the same year, Nurshahiera Rosdi et. al [46]** used steel millscale waste to synthesize $\text{BaMg}_{0.6}\text{Ti}_{0.6}\text{Fe}_{10.8}\text{O}_{19}$ and the powder was heated at $800, 900$ and $1000\text{ }^\circ\text{C}$. XRD results confirmed formation of single phase at $1000\text{ }^\circ\text{C}$. Decrease in magnetic parameters with substitution was observed. Crystallinity of sample found to increases with superexchange interaction. Maximum reflection loss for sample sintered at $1000\text{ }^\circ\text{C}$ was observed (-22.59 dB at 9.42 GHz). **Manju Sharma et al. [47]** also prepared $\text{BaFe}_{12-x}\text{Zn}_{x/2}\text{Zr}_{x/2}\text{O}_{19}$ ($x=0.3, 0.5, 0.7, 1$) using solid state method. To study the effect of heating on properties of Zn- Zr doped barium hexaferrite; powders were sintered in microwave and conventional furnace. Magnetoplumbite phase of composite was achieved faster in microwave (5 min)

then conventional treatment (5 hours) at 1000 °C. Saturation magnetization in case of conventional sintering was found to be 76 emu/g whereas for microwave its value was 104emu/g. Moreover, coercivity decreases drastically from 2961 to 163 Oe in microwave sintered sample.

2.3 Composite Ferrite

In past few years, composites have gained attention due to their phenomenal microwave applications and extensive research has been done to investigate the magnetic and microwave properties in last few decades. This section summarizes the work carried out so far in this purpose.

In the year 2008, F. Tabatabaie et al. [48] synthesized $\text{SrFe}_9\text{Mn}_{1.5}\text{Ti}_{1.5}\text{O}_{19}$ via solid state method. Ferrite polymer (polyvinylchloride matrix) composites were prepared in various ferrite ratios of 50:50, 60:40 and 80:20 and were examined accordingly. The SEM results confirmed existence of magnetoplumbite shaped particles having average size $\sim 2\mu$. The results showed that 70:30 composites had maximum reflection loss at 18.84 GHz with value -26 dB.

In the year 2009, Vijutha Sunny et al. [49] used modified sol-gel technique to prepare nickel ferrite first and ball milled the samples to prepare nickel-rubber nanocomposite. Dielectric properties of composite were studied using cavity perturbation medium and an increase in permittivity with substitution was observed. For 12 mm thick samples, minimum reflection loss was found to be -5.9 dB.

In the same year, Debangsu Roy et al. [19] mixed $\text{BaFe}_{12}\text{O}_{19}$ with $\text{Ni}_{0.8}\text{Zn}_{0.2}\text{Fe}_2\text{O}_4$ to form a composite and studied its structural and magnetic properties. Exchange coupling behavior in nanocomposite was studied at two different temperatures: 400 °C and 800 °C. More profound exchange interactions were found for composite treated at 400 °C. Large area in second quadrant recommended that chemical preparation with proper sintering condition result in developing magnet having high BH_{max} value.

In the year 2012, Yan Wang et al. [50] synthesized $\text{BaFe}_{12}\text{O}_{19}/\text{Ni}_{0.8}\text{Zn}_{0.2}\text{Fe}_2\text{O}_4$ composite using sol-gel technique. Pure phase formation of $\text{BaFe}_{12}\text{O}_{19}/\text{Ni}_{0.8}\text{Zn}_{0.2}\text{Fe}_2\text{O}_4$ was confirmed for temperatures above $800\text{ }^\circ\text{C}$. Magnetic parameters such as coercivity was found to be 2750 Oe while $M_s \sim 63\text{ emu/g}$. At $400\text{ }^\circ\text{C}$, “bee waist” shaped hysteresis for composite got disappear. For ratio 1:5, remanance was found to be higher as compared to pure BaM. **In the next year, S. Manjura Hoque et al. [51]** prepared $\text{BaFe}_{12}\text{O}_{19}/\text{CoFe}_2\text{O}_4/\text{MgFe}_2\text{O}_4$ nanocomposite via co-precipitation route with and without application of ultrasonic vibration. Face-centered cubic and hexagonal structures of soft, hard ferrites were confirmed by XRD analysis. Dependence of coercivity and anisotropy in the range $20 - 700\text{ }^\circ\text{C}$ was studied for both composites. VSM results showed convex $M-H$ curve that indicated strong exchange coupling in BaM/CFO composite. High value of $(\text{BH})_{\text{max}}$ was obtained for $\text{BaFe}_{12}\text{O}_{19}/\text{CoFe}_2\text{O}_4$ composite.

In 2014, Fenfang Xu et al. [52] fabricated chiral polyaniline/barium hexaferrite composite using L-camphor sulfonic acid via in-situ polymerization. Chirality of composite was detected by D-/L-alanine electrolyte. Microwave measurements for PANI/BF composite were carried out in $26.5\text{-}40\text{ GHz}$ range and at 33.25 GHz , minimum reflection loss was -30.5 dB . Such microwave properties of composite indicates towards improvement in impedance matching.

In the year 2015, Haibo Yang et al. [53] used one step chemical method to synthesize $\text{BaFe}_{12}\text{O}_{19}/\text{Y}_3\text{Fe}_5\text{O}_{12}$ nanocomposite and further used in-situ polymerization to coat composite with polyaniline. XRD peaks were obtained for both $\text{BaFe}_{12}\text{O}_{19}/\text{Y}_3\text{Fe}_5\text{O}_{12}$ phases and crystallite size was calculated via Scherrer’s formula. SEM images showed presence of hexagonal and plate like grains corresponding to $\text{BaFe}_{12}\text{O}_{19}$ and $\text{Y}_3\text{Fe}_5\text{O}_{12}$ particles respectively. Microwave properties were investigated and maximum reflection loss was found to be -40.8 dB at 9.9 GHz . **In the next year, Shahab Torkian et al. [54]** prepared a series of $\text{SrFe}_{10}\text{Al}_2\text{O}_{19}/\text{Co}_{0.8}\text{Ni}_{0.2}\text{Fe}_2\text{O}_4$ composite via single pot auto-combustion technique. Data obtained from XRD analysis confirmed presence of $\text{SrFe}_{10}\text{Al}_2\text{O}_{19}$ and

$\text{Co}_{0.8}\text{Ni}_{0.2}\text{Fe}_2\text{O}_4$ phases. Hexagonal platelet with spheres corresponds to $\text{SrFe}_{10}\text{Al}_2\text{O}_{19}$ and $\text{Co}_{0.8}\text{Ni}_{0.2}\text{Fe}_2\text{O}_4$ nanoparticles. Smooth hysteresis loop confirmed the strong coupling interaction among soft and hard phases. Highest M_r/M_s ratio (~ 0.63) was obtained for composite having 15% soft phase. They concluded that in comparison to physical mixing, single-pot method had provided better results. **Further, V. Harikrishnan et al. [55]** prepared $(\text{Ba}_{0.5}\text{Sr}_{0.5}\text{Fe}_{12}\text{O}_{19})_{1-x}/\text{CoFe}_2\text{O}_4$ ($x = 0.1- 0.3$) by single step combustion method. TGA results showed decomposition in 3 states and an exothermic peak at 210 °C. Maximum H_c for composite was found to be 4.7 KOe and saturation M_s 60.4 emu/g. With increase in concentration of soft phase, initially exchange coupling increases and then sudden decrease was observed.

In the year 2017, Chhavi Pahwa et al. [56] used two different routes (single pot and physical mixing) to synthesize a nanocomposite of $\text{BaFe}_{12}\text{O}_{19}/\text{NiFe}_2\text{O}_4$ and compared their properties. Microwave properties of $\text{BaFe}_{12}\text{O}_{19}/\text{NiFe}_2\text{O}_4$ nanocomposite were investigated in Ku-band. Smooth hysteresis loop was obtained for composite synthesized via single pot method whereas a kink was obtained in physically mixed composite. Saturation magnetization in exchange coupled composite was higher (57.7 emu/g) than non coupled composite (50.6 emu/g). Exchange coupled material shows R_L at various frequency which was absent in second case. **In the consecutive year, Sachin Tyagi et al. [57]** prepared $\text{BaFe}_{12}\text{O}_{19}/\text{NiFe}_2\text{O}_4$ nanocomposite particles via modified flux technique and synthesized powder was annealed in N_2 environment at 800, 1000 and 1200 °C . SEM results for 1200 °C sintered particles confirmed hexagonal plate like structure with average size of 85-95 nm. At 1200 °C, high saturation magnetization of 55.18 emu/g was obtained. Further, reflection loss (maximum) was found to be -27.1 dB at 11.79 GHz. **In recent publication, Chhavi Pahwa et al. [58]** used sol-gel combustion route to synthesize $\text{BaFe}_{12}\text{O}_{19}/\text{Ni}_{0.5}\text{Zn}_{0.5}\text{Fe}_2\text{O}_4$ nanocrystalline composite having 70/30 hard to soft ratio. Composites were annealed at various temperatures ranging from 950°C to 1150°C. XRD peaks

confirmed the presence of both the phases. Hexagonal and circular shaped particles were seen in TEM micrographs. Magnetic measurements were performed and M_s was found to increase from 58 to 65emu/g while coercivity decreases. For sample annealed at 1050 °C, maximum R_L was found to be -38 dB. During frequency measurements, a shift in loss frequency was observed with temperature.

Chapter 3

Experimental Details

Overview

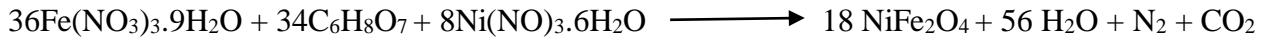
This chapter addresses the processing technique used for the preparation of NiFe_2O_4 , $\text{SrFe}_{12}\text{O}_{19}$ and series of SrM/NiF nanocomposite. Further, a brief description regarding characterization techniques used to study structural and magnetic properties of ferrites has been given.

This experimental section is divided in three major parts as listed below:

1. Synthesis of soft ferrite (NiFe_2O_4).
2. Synthesis of hard ferrite ($\text{SrFe}_{12}\text{O}_{19}$).
3. Synthesis of hard/soft ($\text{SrFe}_{12}\text{O}_{19}/\text{NiFe}_2\text{O}_4$)nanocomposite

3.1 Synthesis of Soft ferrite (NiFe_2O_4) powder

NiFe_2O_4 (NiF) powder was prepared by sol-gel auto combustion method. High purity (99.9 %) citric acid ($\text{C}_6\text{H}_8\text{O}_7$), nickel nitrate ($\text{Ni}(\text{NO}_3)_3 \cdot 6\text{H}_2\text{O}$) and iron nitrate ($\text{Fe}(\text{NO}_3)_3 \cdot 9\text{H}_2\text{O}$) were used. Precursors were mixed in following stoichiometric ratio:

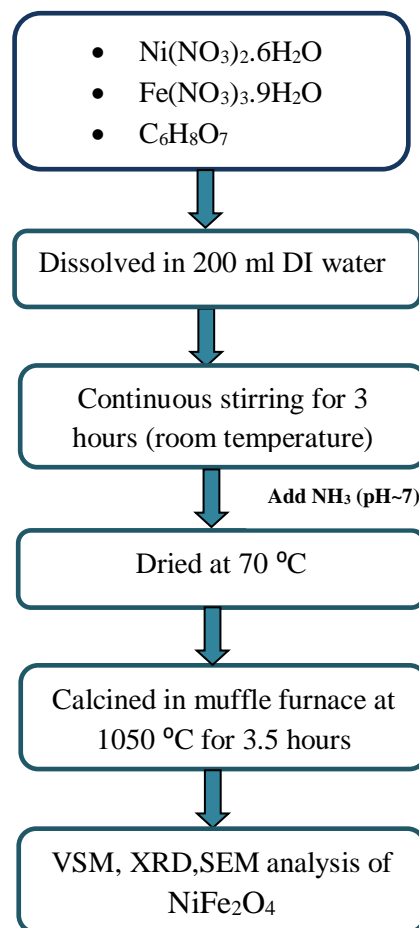


Metal nitrates and citric acid were added in distilled water with constant stirring using magnetic stirrer to obtain homogeneous solution. Once the precursors were dissolved completely in solvent, ammonia (NH_3) was added drop wise to adjust pH ~ 7 of the solution. The resulting solution was allowed to heat at constant temperature (70°C) until spontaneous ignition took place. After combustion, dendritic ash flakes of nickel ferrite were obtained as shown in [fig. 3.1](#). These flakes were further grinded in mortar-pestle to obtain fine powder. Resultant fined ferrite powder was calcined at 1050°C in Muffle furnace for 3.5 hours.



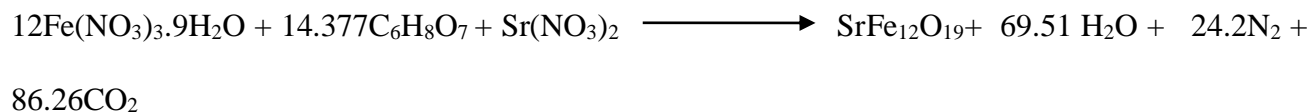
Fig. 3.1 Dendritic ash flakes of ferrite

3.1 Flow chart for synthesis of Nickel Ferrite (NiFe_2O_4) by sol-gel auto combustion method



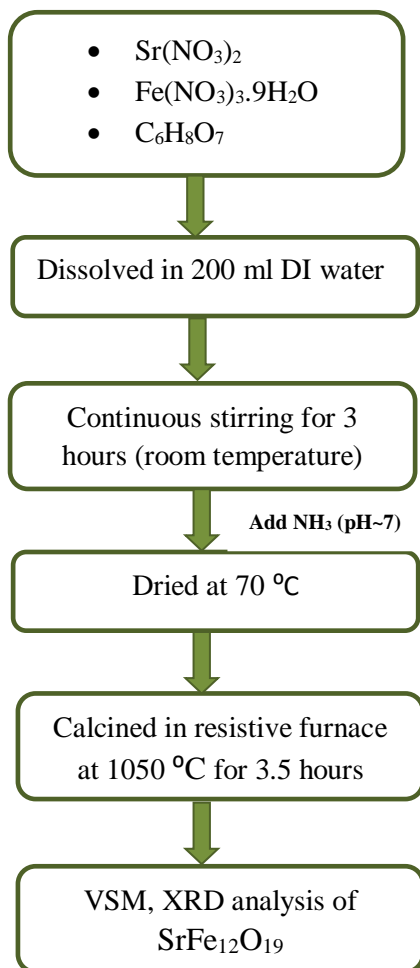
3.2 Synthesis of Hexaferrite (SrFe₁₂O₁₉) powder

SrFe₁₂O₁₉ (SrM) powder was prepared by sol-gel auto combustion method. High purity (99.9 %) citric acid (C₆H₈O₇), strontium nitrate (Sr(NO₃)₂) and iron nitrate (Fe(NO₃)₃.9H₂O) were used. Precursors were mixed in following stoichiometric ratio:



SrFe₁₂O₁₉ powder was obtained by following same procedure as mentioned in section 3.1

2.2 Flow chart for synthesis of Strontium ferrite (SrFe₁₂O₁₉) by sol-gel auto combustion method



3.3 Synthesis of $\text{SrFe}_{12}\text{O}_{19}/\text{NiFe}_2\text{O}_4$ (SrM/ NiF) composite

$(100-x)\text{SrM} + x\text{NiF}$ ($x = 0, 20, 30, 40, 50$) composites were prepared by physical mixing method. The mixture of SrM and NiF was wet milled in acetone media using planetary ball mill with constant powder to ball ratio (1:4). The whole process continued for 3 hours at constant rpm ~ 118 for the homogeneous mixing of two phases.



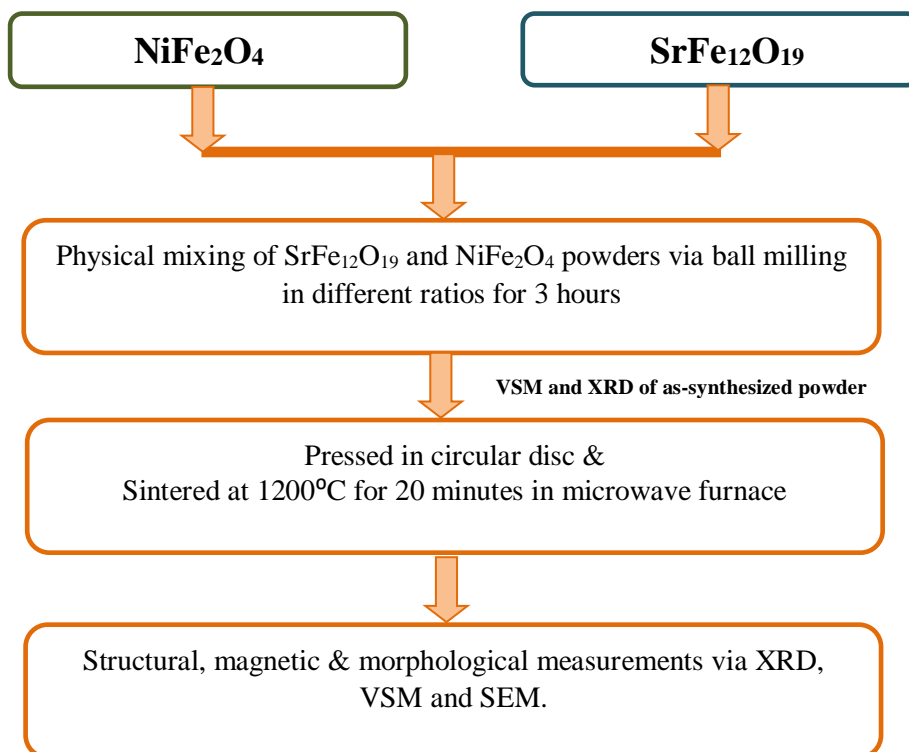
Fig. 3.2 Rotatory Ball mill and Zirconia jar with balls

Resulting slurry was allowed to dry at room temperature. Obtained composite powder was directly used for magnetic and structural analysis. 5 wt % of PVA was added as binder in the sample and then pelletized under the pressure of 50MPa. These pellets were further sintered at 1200 °C for 20 minutes in microwave furnace.



Fig. 3.3 Microwave furnace

3.2 Flow chart for synthesis of SrM/ NiF composite by physical mixing method



3.4 Characterization technique

Prepared pure NiF, SrM and nanocomposites of SrM/NiF with different weight ratios (80/20, 70/30, 60/40,50/50) were analyzed to study the structural, magnetic and morphological properties.

Three main instrumentations were used for the analysis as listed below.

1. X-ray Diffractometer

To confirm single phase formation in SrFe₁₂O₁₉, NiFe₂O₄ and composite, Panalytical's X'Pert pro XRD instrument was used. Cu K_{α1} radiation having wavelength 1.54 Å was used for analysis along with Ni metal filter. Phase analysis was carried out in range of 20-80 degree (2θ) with 0.02 degree scanning step.

2. Vibrating Sample Magnetometer

To analyze the magnetic properties of pure SrM, NiF and SrM/NiF nanocomposite, Lake shore 7404 VSM instrument was used. Magnetic field in the range of -10000 to 10000 Oe was applied at room temperature to study magnetic behavior of samples.

3. Scanning Electron Microscope

Surface morphology of SrM/NiF nanocomposite was determined using JOEL (JSM-1T100) SEM instrument. Prior to measurement sample surface were coated with gold using sputtering to avoid charging of the sample that occurs due to accumulation of static field.

Chapter 4

Results and Discussion

Overview

Firstly, XRD analysis of SrFe₁₂O₁₉, NiFe₂O₄ and their compositions were discussed. Further, the magnetic behavior of powder as well as sintered composite was investigated using Vibrating Sample Magnetometer (VSM). Lastly, Scanning Electron Microscope (SEM) analysis was performed to investigate microstructure of SrFe₁₂O₁₉, NiFe₂O₄ and their compositions.

4.1 X-Ray Diffraction (XRD)

XRD patterns of pure strontium ferrite (SrM), nickel ferrite (NiF) and SrM/NiF nanocomposite (70/30) prepared by physical mixing method are shown in [fig. 4.1](#). In pure NiF and SrM, all XRD peaks correspond to spinel (NiFe_2O_4) and hexagonal ($\text{SrFe}_{12}\text{O}_{19}$) phases without any impurity. In the SrM/NiF composite system; diffraction peaks confirm the co-existence of both hexagonal (SrM) and spinel (NiF) phases. No traces of any impurity or secondary phase were obtained in the respective XRD patterns.

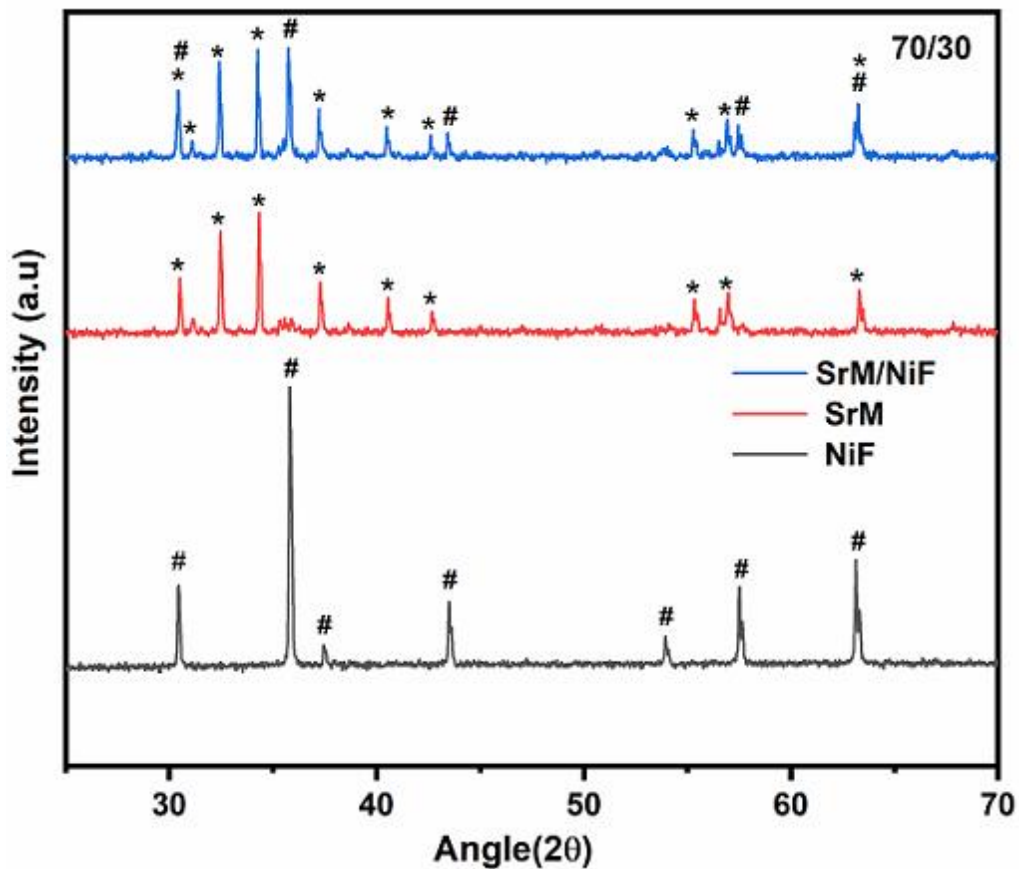


Fig. 4.1 XRD pattern of pure NiF, SrM and SrM/NiF (70/30) nanocomposite

The average crystallite size for SrM and NiF in pure and composite samples was calculated by Scherrer formula [59] given as:

$$t = \frac{k\lambda}{\beta \cos \theta} \quad (1)$$

where, t : crystallite size, k : Scherrer constant (0.9), λ : wavelength of incident radiation (1.54 Å), β : FWHM (full width half maxima) of corresponding XRD peak, θ : Bragg's angle.

The obtained crystallite size for SrM and NiF in composite are tabulated in [table 4.1](#). Average crystallite size for SrM and NiF in pure and composite samples is found to be nearly same.

Table 4.1 Crystallite size of SrM and NiF for pure and composite powder

Sample	Crystallite size (nm)	
SrM	63.02	
NiF	52.13	
SrM/NiF (70/30)	SrM- 61.6	NiF- 50.8

[Fig. 4.2](#) shows XRD pattern of microwave sintered SrM/NiF composite pulverized powder to study the affect of microwave sintering on crystallite size. From the figure, it is clear that both SrM and NiF phases were also co-exist in the composite after sintering. No secondary phase formation was observed. The average crystallite for microwave sintered pure SrM (29.6nm) and SrM/NiF (23.34 / 21.79 nm) composite found to decrease. This suggests that microwave sintering refine the crystallite size without any grain coarsening.

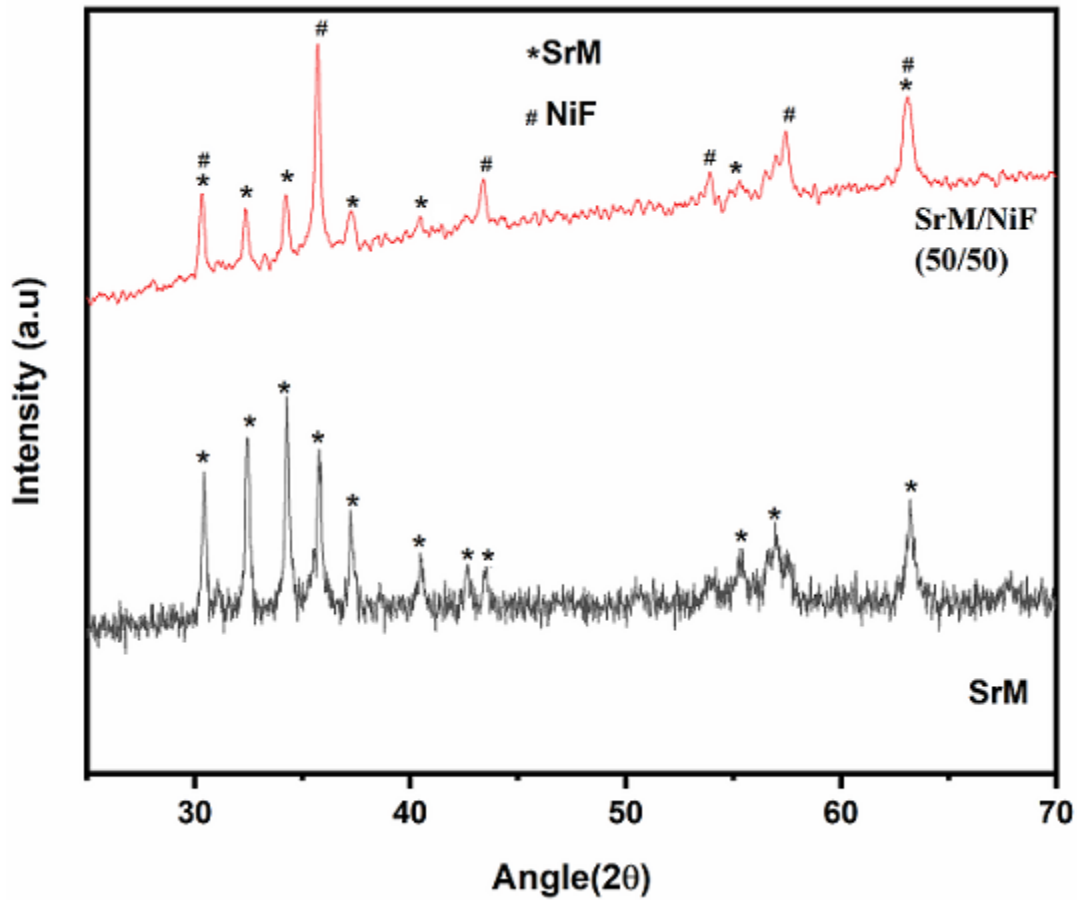


Fig. 4.2 XRD pattern of microwave sintered SrM and SrM/NiF (50/50) nanocomposite

4.2 Magnetic Measurements

M-H loop of as-synthesized nickel ferrite (NiF), strontium ferrite (SrM) and SrM/NiF (80/20, 70/30, 60/40, 50/50) nanocomposite prepared by physical mixing are shown in [fig.4.3 \(a & b\)](#). SrM and NiF showed their characteristic *M-H* behavior of hard and soft ferrite with M_s : 56.93 & 46.52 emu/g and H_c : 2140.48 & 92.19 Oe respectively [6,9].

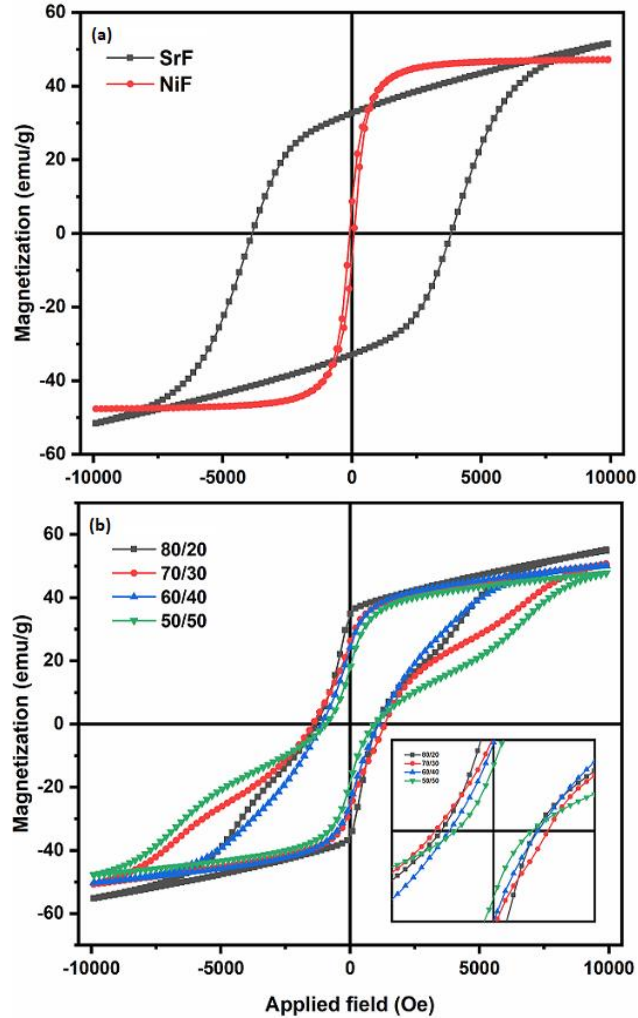


Fig. 4.3 *M-H* loops of (a) SrM & NiF, and (b) physically mixed SrM/NiF nanocomposite powders.

Fig. 4.3 (b) shows the representative *M-H* loops of SrM/NiF composite powder in different weigh fraction prepared by physical mixing method. Stepped *M-H* loop were obtained for all composition of SrM/NiF composites. It is well reported that such system with kink in demagnetization curve corresponds to non-exchange couple system [18]. As three types of interfacial interaction exist in the composite system: between soft-soft phase, hard-hard phase and hard-soft phase. The obtain kink in demagnetization curve correspond to individual switching of hard and soft phase with applied field. The

kink becomes more pronounced with the NiF content (inset 4.3(b)). Such switching takes place when individual spin interaction dominates over interfacial interactions.

Fig. 4.4 (a & b) showed the variation in M_s and H_c with NiF content in physically mixed SrM/NiF composite. Theoretical values for M_s and H_c were also calculated by rule of mixture using following equation [60] and compared with experimental values:

$$M_c = (1-x)M_{SrM} + xM_{NiF} \quad (2)$$

where, M_{SrM} , and M_{NiF} represents measured M_s of SrM (56.93 emu/g) and NiF (46.52 emu/g) respectively. Similarly, H_c for the composite for different weight content of NiF was calculated and compared to experimental values.

From the fig. 4.4 (a), it is clear that M_s of the composite decrease with the NiF content. The decrease in magnetization of the composite is the consequence of non-exchange coupling between hard/soft phase as confirmed by demagnetization curve of $M-H$ loop. The low M_s of NiF is also responsible for decrease in magnetization of non-exchange coupled composite with the NiF content. Experimental M_s of the composites also lags behind to the theoretical calculated M_s which also confirms the insufficient coupling between SrM and NiF phases. It is well reported that for exchange coupled system M_s of the composite should be higher than theoretical magnetization calculated by rule of mixture (equation 2) [58].

H_c of the composite also found to decrease with the NiF content but lie near to theoretical calculated value. The decrease in coercivity of the composite with the NiF content is due to dominance of soft magnetic nature of the NiF [19].

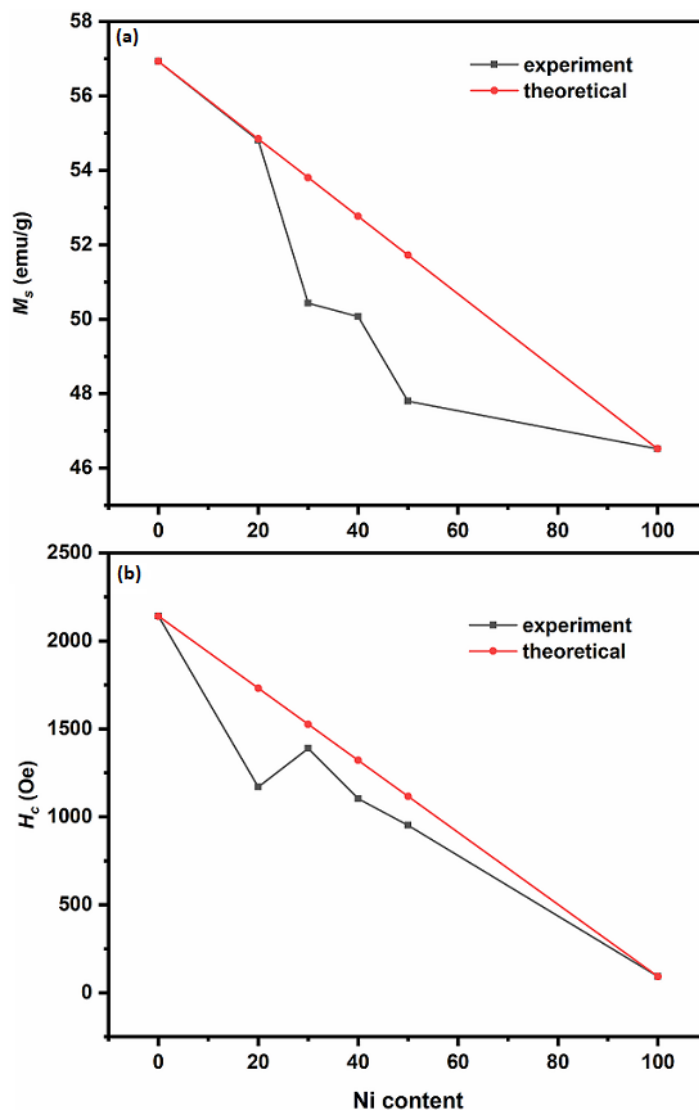


Fig. 4.4 Variation in theoretical and experimental observed (a) M_s and (b) H_c of SrM/NiF nanocomposite with NiF content

Further, as-synthesized pure and composite powders were pressed into pellets and microwave sintered at 1200 °C for 20 minutes. Effect of sintering on exchange coupling and magnetic characteristics of NiF, SrM and SrM/NiF nanocomposite were observed and plotted in [fig. 4.5 \(a & b\)](#).

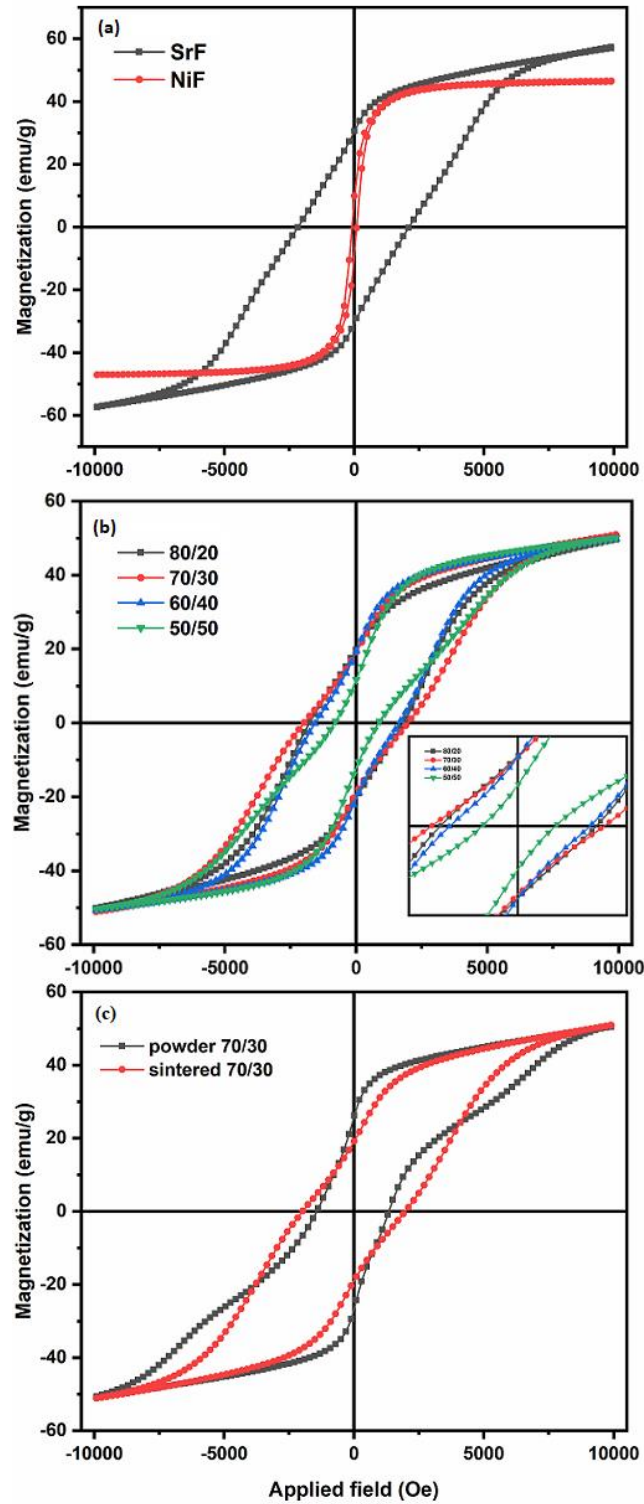


Fig. 4.5 *M-H* loop of sintered (a) SrM and NiF (b) SrM/NiF nanocomposite with different composition (c) powder and sintered 70/30 composite

M - H loops of sintered SrM and NiF (fig 4.5(a)) also shows the characteristic behavior of hard and soft phase. High M_s (51.6 emu/g) and H_c (3848 Oe) of the sintered SrM compared to NiF are in agreement with the previous reported values [61, 62].

M - H loops of microwave sintered composites are shown in fig. 4.5(b). A small kink or shoulder was also obtained in the sintered composite for all compositions. However, the kink is less prominent (inset 4.5(b)) as compared to as mixed composites (inset 4.3(b)). The fig. 4.5 (c) shows the representative comparison of powders and sintered magnets. The small kink in demagnetization curve of sintered sample suggests that fraction of coherent spin rotation is increased. Therefore, microwave sintering enhances exchange-coupling between hard and soft phases.

Fig. 4.6 (a & b) showed variation in experimental and theoretical calculated M_s and H_c of SrM/NiF nanocomposite with NiF content. From the fig.4.6 (a), it is clear that experimental obtained M_s of the composite nearly equal to the theoretical calculated values. For 70/30, 50/50 composition, M_s of the composites are slightly higher than the theoretical calculated which indicates coupling between hard and soft phase increases after microwave heat treatment. While continuous decrease in H_c for all sintered composites is due to soft magnetic nature of NiF.

It was also observed that sintered M_s of pure and composite samples were smaller than the as mixed powder composites. This might be due to the deficiency of ambient atmosphere and oxygen ions in the microwave furnace which results in conversion of Fe^{3+} ions into Fe^{2+} ions hence results reduction in magnetization of pure and composite ferrites.

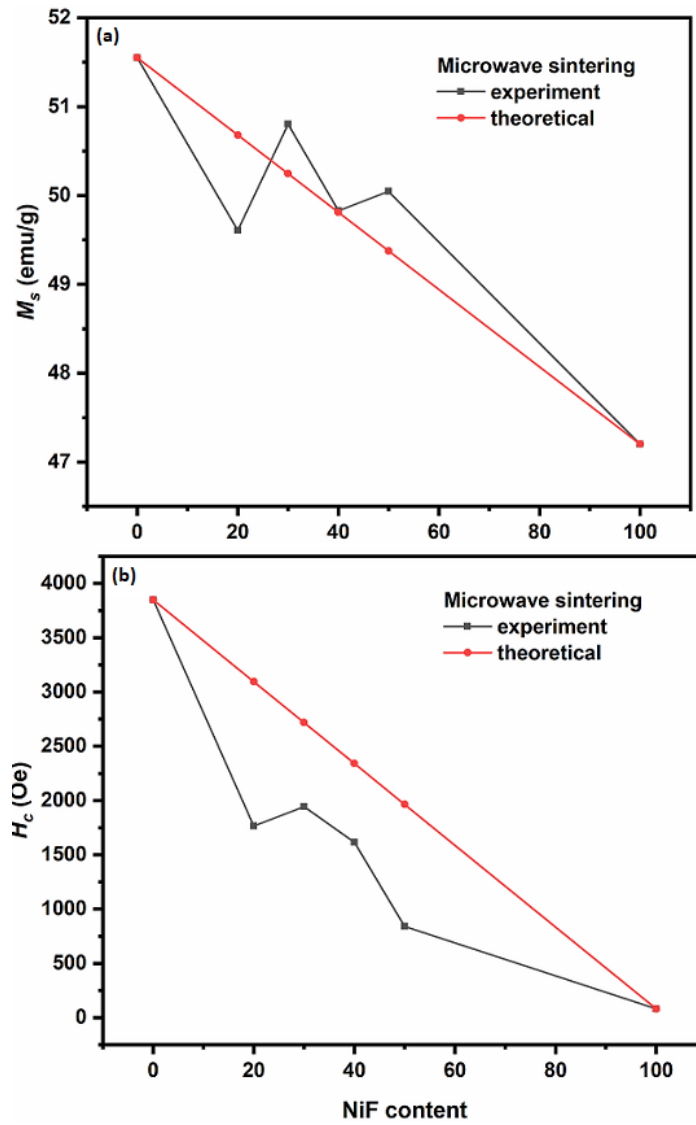


Fig. 4.6 Variation in theoretical and experimental observed (a) M_s and (b) H_c of SrM/NiF nanocomposite with NiF content sintered at 1200 °C

4.3 Scanning Electron Microscope (SEM)

NiF, SrM and SrM/NiF (80/20, 70/30, 60/40, 50/50) powders were pressed into pellets and microwave sintered at 1200 °C. Fig. 4.7 (a-c) represents fractured surface micrographs of NiF, SrM and SrM/NiF (70/30) nanocomposite. Microstructure of pure NiF shows nearly spherical grains. The microstructure of SrM also shows smaller grains with limited porosity. Fig. 4.7 (c) shows the microstructure of composites where small and large grains are well separated. The grains are dense packed without any porosity, which suggest that composite are well sintered.

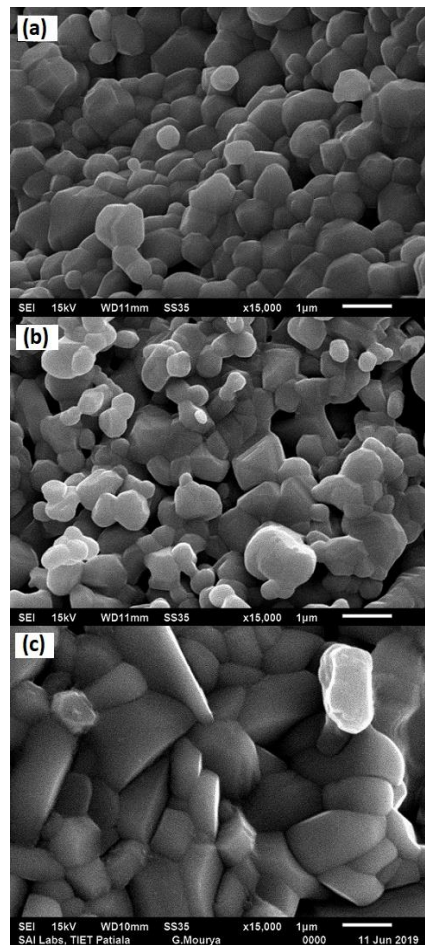


Fig. 4.7 SEM micrographs of (a) NiF (b) SrM and (c) SrM/NiF (70/30) sintered at 1200 °C

CONCLUSION

Microwave sintered NiFe_2O_4 (NiF), $\text{SrFe}_{12}\text{O}_{19}$ (SrM) and nanocomposite of SrM/NiF in different weight ratios (80/20, 70/30, 60/40, 50/50) were successfully prepared by physical mixing of individual NiF and SrM powder. The effect of relative weight fraction on structural, morphological and magnetic properties was investigated. Co-existence of both soft (NiFe_2O_4) and hard ($\text{SrFe}_{12}\text{O}_{19}$) phases was confirmed by XRD analysis. Average crystallite size for NiF, SrM and SrM/NiF was found to decrease with sintering. Stepped M - H loop were obtained for all composition of SrM/NiF composites while less prominent kink was observed in sintered SrM/NiF nanocomposites. Experimental M_s of the composites lags behind to the theoretical calculated M_s which confirms the insufficient coupling between SrM and NiF phases. For 70/30, 50/50 composition, M_s of the composites was slightly higher than the theoretical calculated which indicates increases in coupling after microwave heat treatment.

REFERENCES

- [1] John Jacob, M Abdul Khadar, Anil Lonappan and K T Mathew, “Microwave dielectric properties of nanostructured nickel ferrite”, *Bull. Mater. Sci.* 31 (2008) 847-851.
- [2] Umit Ozgur, Yahya Alivov, Hadis Morkoc, “Microwave ferrites, part 1: fundamental properties”, *Journal of Material Science: Mater Electron* (2009) 20:789-834
- [3] Zeynep Karcioglu Karakas, Recep Boncukcuoglu, Ibrahim Hakki Karakas, Mehmet Ertugrul, “The effects of heat treatment on the synthesis of nickel ferrite (NiFe₂O₄) nanoparticles using the microwave assisted combustion method”, *Journal of Magnetism and Magnetic Materials* 374 (2015) 298-306
- [4] Vincent G. Harris, Anton Geiler, Yajie Chen, Soack Dae Yoon, Mingzhong Wu, Zhaohui Chen, Peng He, Patanajali V. Parimi, Xu Zuo, Carmine Vittoria, “Recent advances in processing and applications of microwave ferrite”, *Journal of Magnetism and Magnetic Materials* 321(2009) 2035-2047
- [5] Raul Valenzuela, “Novel Applications of Ferrites”, *Physics Research International* 2012 (2011) Article ID 591839, 9 pages.
- [6] M. Kooti, A. Naghdi Sedeh, “Synthesis and Characterization of NiFe₂O₄ magnetic nanoparticles by combustion method”, *J. Mater. Sci. Technol.* 29(1) (2013) 34-38
- [7] Ayaz Arif Khan, M. Javed, A. Rauf Khan, Yousaf Iqbal, Asif Majeed, Syed Zahid Hussain, S.K. Durrani, “Influence of preparation method on structural, optical and magnetic properties of nickel ferrite nanoparticles”, *Materials Science-Poland*, 35(1) (2017) 58-65

- [8] Vincent G. Harris, "Modern microwave ferrites", IEEE Transactions on magnetic 48 (2012) 1075-1104
- [9] F.N.Tenorio Gonzalez, A.M.Bolarín Miro, F.Sánchez De Jesus, C.A.Cortes Escobedo, S.Ammar, "Mechanism and microstructural evolution of polyol mediated synthesis of nanostructured M-type $\text{SrFe}_{12}\text{O}_{19}$ ", Journal of Magnetism and Magnetic Materials 407 (2016) 188-194
- [10] Hossein Nikmanesh, Sedigheh Hoghoghifard, Behnaz Hadi-Sichani, "Study of the structural, magnetic, and microwave absorption properties of the simultaneous substitution of several cations in the barium hexaferrite structure", Journal of Alloys and Compounds 775 (2019),1101-1108
- [11] Robert C. Pullar, "Hexagonal ferrites: A review of the synthesis, properties and applications of hexaferrite ceramics", Progress in Material science 57 (2012) 1191-1334
- [12] Izadkhah, H.Zare, S.Somu, S.Lombardi, Vittoria, "Utilizing alternate target deposition to increase the magnetoelectric effect at room temperature in a single phase M-type hexaferrite", MRS Communications 7(2) (2017) 97-101.
- [13] Eric E. Fullerton, J.S. Jiang, S.D Bader, "Hard/soft hetrostructures: model exchange-spring magnets", Journal of Magnetism and Magnetic Materials 200 (1999) 392-404
- [14] Joseph E. Davies, Olav Hellwig, J.S. Jiang, S.D. Bader, G.T. Zimanyi and Kai Liu, "Anisotropy dependence of irreversible switching in Fe/SmCo and FeNi/FePt exchange spring magnet films", Applied Physics Letters 86 (2005), 262503
- [15] G. Sarriegui, J.M. Martin, M.Ipatov, A.P. Zhukov and J. Gonzalez, "Magnetic properties of NdFeB alloys obtained by gas atomization technique", IEEE transactions on magnetic (2018) 9464

- [16] Debangsu Roy, K.V. Sreenivasulu, P. S. Anil Kumar, “Investigation on non exchange spring behaviour and exchange spring behaviour: A first order reversal curve analysis”, Applied Physics Letters 103 (2013) 222406
- [17] Debangsu Roy, C Shivakumara and P. S. Anil Kumar, “On the magnetization reversal of oxide based exchange spring magnet”, Journal of Applied Physics 109 (2011) 07A761
- [18] Haibo Yang, Ting Ye, Ying Lin, Miao Liu, “Excellent microwave absorption property of ternary composite: PolyanilineBaFe₁₂O₁₉-CoFe₂O₄ powders”, Journal of Alloys and Compounds 653 (2015) 135-139
- [19] Debangsu Roy, K.V. Sreenivasulu, P. S. Anil Kumar, “Observation of the exchange spring behavior in hard-soft-ferrite nanocomposite”, Journal of Magnetism and Magnetic Materials 321 (2009) L11- L14
- [20] R. K. Kotnala, Shahab Ahmad, Arham S. Ahmed, Jyoti Shah and Ameer Azam, “Investigation of structural, dielectric, and magnetic properties of hard and soft mixed ferrite composites”, Journal of Applied Physics 112 (2012) 054323
- [21] J.S. Ghodake, Rahul C. Kamble, T.J Shinde, P.K Maskar, S.S Suryavanshi, “Magnetic and microwave absorbing properties of Co²⁺ substituted nickel zinc ferrites with emphasis on initial permeability studies”, Journal of Magnetism and Magnetic Materials 401(2016)938-942.
- [22] C.S. Pawar, M. P. Gujar, V. L. Mathe “Optical Properties of Spin-Deposited Nanocrystalline Ni-Zn Ferrite Thin Films Processed by Sol-Gel”, J Supercond Nov Magn (2017) 30:615–625.
- [23] F.Licci, G. Turilli and T.Besagn, “Phase Analysis and Single Domain Detection in Hexaferrite Powders for Magnetic Recording”, IEEE Transactions on Magnetics 24 (1988) 593-597

- [24] J.F. Wang, C.B. Ponton, I.R. Harris, “Ultrafine SrM particles with high coercivity by chemical coprecipitation”, *Journal of Magnetism and Magnetic Materials* 242–245 (2002) 1464–1467
- [25] A. Ataie, I. R. Harris, C. B. Ponton, “Magnetic properties of hydrothermally synthesized strontium hexaferrite as a function of synthesis conditions”, *Journal of Materials Science* 30 (1995) 1429-1433
- [26] M.A. El Hiti, “Dielectric behavior and ac electrical conductivity of Zn-substituted Ni-Mg ferrites”, *Journal of Magnetism and Magnetic Materials* 164 (1996) 187- 196
- [27] Anjali Verma and Dinesh C. Dube, “Processing of Nickel–Zinc Ferrites Via the Citrate Precursor Route for High-Frequency Applications”, *J. Am. Ceram. Soc.*, 88 [3] 519–523 (2005)
- [28] C. P. L. Rubinger, D. X. Gouveia, J. F. Nunes, C. C. M. Salgueiro, J. A. C. Paiva, M. P. F. Graca, P. Andre and L. C. Costa, “Microwave dielectric properties of NiFe₂O₄”, *Microwave and Optical Technology Letters* ,Vol. 49,1341-1343 (2007)
- [29] M. Sertkol, Y. Koseoglu, A. Baykal, H. Kavas, A. Bozkurt, M.S. Toprak, “Microwave synthesis and characterization of Zn-doped nickel ferrite nanoparticles”, *Journal of Alloys and Compounds* 486 (2009) 325-329
- [30] Xuegang Lu, Gongying Liang, Qianjin Sun, Caihua Yang, “High-frequency magnetic properties of Ni-Zn nanoparticles synthesized by a low temperature chemical method”, *Materials Letters* 65 (2011) 674-676
- [31] M. Ognjanovic, Ivan Tokic, Zeljka Cvejic, Srdjan Rakic, Vladimir V. Srdic, “ Structural and dielectric properties of yttrium substituted nickel ferrites”, *Materials Research Bulletin* 49 (2014) 259-264

- [32] M. Penchal Reddy ,W. Madhuri ,K. Sadhana, I. G. Kim ,K. N. Hui ,K. S. Hui ,K. V. Siva Kumar ,R. Ramakrishna Reddy, “Microwave sintering of nickel ferrite nanoparticles processed via sol–gel method”, J Sol-Gel Sci Technol (2014) 70:400–404
- [33] Ch. Srinivas, B.V.Tirupanyam, S.S.Meena, S.M.Yusuf, Ch.SeshuBabu, K.S. Ramakrishna, D.M.Potukuchi, D.L.Sastry, “Structural and magnetic characterization of co-precipitated $Ni_xZn_{1-x}Fe_2O_4$ ferrite nanoparticles”, Journal of Magnetism and Magnetic Materials 407(2016)135–141
- [34] S. Deepak Ram Prasath, S. Balaji, S. Raju, V. Abhaikumar, “Synthesis and characterization of zinc substituted nickel ferrite materials for L band antenna applications”, J Mater Sci: Mater Electron (2016) 27:8247–8253
- [35] G. Umaphathy, G. Senguttuvan, L. John Berchman, V. Sivakumar, “Structural, dielectric and AC conductivity studies of Zn substituted nickel ferrites prepared by combustion technique”, J Mater Sci: Mater Electron (2016) 27:7062–7072.
- [36] R. Muller, H. Pfeiffer, W. Schuppel, “Variation of the magnetic properties of barium ferrite powders by heat treatment”, J Magnetism and Magnetic Materials 101 (1991)237-238
- [37] H. Pfeiffer, R.W. Chantrell , P. Gornert, W. Scuijffel , E. Sinn, M. Rosler, “Properties of barium hexaferrite powders for magnetic recording”, Journal of Magnetism and Magnetic Materials 125 (1993) 373-376
- [38] C. Surig, K.A. Hempel, D. Bonnenberg, “Hexaferrite particles prepared by sol-gel technique”, IEEE Transactions on Magnetics 30 (1994) 4092-4094

- [39] Sachin Tyagi, Ramesh Chandra Agarwala, Vijaya Agarwala, “Reaction kinetic, magnetic and microwave absorption studies of $\text{SrFe}_{11.2}\text{Ni}_{0.8}\text{O}_{19}$ hexaferrite nanoparticles”, *J Mater Sci: Mater Electron* (2011) 22:1085–1094
- [40] S. Kanagesan, S. Jesurani, R. Velmurugan, M. Sivakumar, C. Thirupathi, T. Kalaivani, “Synthesis and magnetic properties of conventional and microwave calcined barium hexaferrite powder”, *J Mater Sci: Mater Electron* (2012) 23:635–639
- [41] Z.Mosleh, P.Kameli, A.Poorbaferani, M.Ranjbar, H.Salamati, “Structural, magnetic and microwave absorption properties of Ce-doped barium hexaferrite”, *Journal of Magnetism and Magnetic Materials* 397 (2016) 101-107
- [42] Qian Liu Yingli Liu, Chongsheng Wu, Yu Wang, Jie Li Liwen Gao, Huaiwu Zhang, “Investigation on Zn-Sn co-substituted M-type hexaferrite for microwave applications”, *J. Magn. Magn. Mater*, 444 (2017) 421-425
- [43] Hossein Nikmanesh, Mahmood Moradi, Gholam Hossein Bordbar, Reza Shams Alam, “Effect of multi dopant barium hexaferrite nanoparticles on the structural, magnetic, and X-Ku bands microwave absorption properties”, *Journal of Alloys and Compounds* 708 (2017) 99-107
- [44] Jianfeng Chen, Yu Wang, Yingli Liu, Haoxian Wang, Qian Liu, Yanjun Chen, “Investigation of oriented Co^{3+} doped M-type hexaferrite $\text{Sr}_{0.5}\text{Ba}_{0.5}\text{Fe}_{12-x}\text{Co}_x\text{O}_{19}$ for microwave application”, *Journal of Materials Science: Materials in Electronics* (2018) 29:14371–14377
- [45] Santhoshkumar Mahadevana, Sukhleen Bindra Narang, Puneet Sharma, “Effect of three-step calcination on structural, magnetic and microwave properties of $\text{BaFe}_{11.5}\text{Ti}_{0.5}\text{O}_{19}$ hexaferrite”, *Ceramic International* (2019) 45, 9000-9006

- [46] Nurshahiera Rosdi, Rabaah Syahidah Azis, Muhammad Syazwan Mustaffa, Nor Hapishah Abdulla, Syazana Sulaiman, Tan Tong Ling, “Synthesis and characterization of Mg–Ti substituted barium hexaferrite ($\text{BaMg}_{0.6}\text{Ti}_{0.6}\text{Fe}_{10.8}\text{O}_{19}$) derived from millscale waste for microwave application”, *Journal of Materials Science: Materials in Electronics* (2019) 30:8636–8644
- [47] Manju Sharma, Subhash C. Kashya, “Improvement in magnetic parameters of polycrystalline barium hexaferrite by nonmagnetic cation substitution and microwave processing”, *Ceramics International* (2019) 45,11226-11232
- [48] F. Tabatabaie, M.H. Fathi, A.Saatchi, A. Ghasemi, “Microwave absorption properties of Mn- and Ti-doped strontium hexaferrite”, *Journal of Alloys and Compounds* 470 (2009) 332-335
- [49] Vijutha Sunny, Philip Kurian, P. Mohanan, P.A.Joy, M.R. Anantharaman, “A flexible microwave absorber based on nickel ferrite nanocomposite”, *Journal of Alloys and Compounds* 489 (2010) 297-303
- [50] Yan Wang, Ying Huang, Qiufen Wang, “Preparation and magnetic properties of $\text{BaFe}_{12}\text{O}_{19}/\text{Ni}_{0.8}\text{Zn}_{0.2}\text{Fe}_2\text{O}_4$ nanocomposite ferrite”, *Journal of Magnetism and Magnetic Materials* 324 (2012) 3024-3028
- [51] S. Manjura Hoque, C. Srivastava, V.Kumar, N. Venkatesh, H.N. Das, D.K. Saha, K.Chattopadhyay, “Exchange-spring mechanism of soft and hard ferrite nanocomposites”, *Materials Research Bulletin* 48 (2013) 2871-2877.
- [52] Fenfang Xu, Li Ma, Mengyu Gan, Jihai Tang, Zhitao Li, Jiyue Zheng, Jun Zhang, Shuang Xie, HuiYin, Xiaoyu Shen, Jinlong Hu, Feng Zhang, “Preparation and characterization of chiral polyaniline/barium hexaferrite composite with enhanced microwave absorbing properties”, *Journal of Alloys and Compounds* 593 (2014) 24–29

- [53] Haibo Yang, Ting Ye, Ying Lin, Miao Liu, “Exchange coupling behavior and microwave absorbing property of hard/soft ($\text{BaFe}_{12}\text{O}_{19}/\text{Y}_3\text{Fe}_5\text{O}_{12}$) ferrites based on polyaniline”, *Synthetic Metals* 210 (2015) 245-250
- [54] Shahab Torkian, Ali Ghasemi, Reza Shoja Razavi, “Magnetic properties of hard-soft $\text{SrFe}_{10}\text{Al}_2\text{O}_{19}/\text{Co}_{0.8}\text{Ni}_{0.2}\text{Fe}_2\text{O}_4$ ferrite synthesized by one pot sol gel auto-combustion”, *Journal of Magnetism and Magnetic Materials* 416 (2016) 408-416
- [55] V. Harikrishnan, R. Ezhil Vizhi, “A study on the extent of exchange coupling between $(\text{Ba}_{0.5}\text{Sr}_{0.5}\text{Fe}_{12}\text{O}_{19})_{1-x}/(\text{CoFe}_2\text{O}_4)$ magnetic nanocomposites synthesized by sol-gel combustion method”, *Journal of Magnetism and Magnetic Materials* 418 (2016) 217-223
- [56] Chhavi Pahwa, Santhoshkumar Mahadevan, Sukhleen Bindra Narang, “Structural, magnetic and microwave properties of exchange coupled $\text{BaFe}_{12}\text{O}_{19}/\text{NiFe}_2\text{O}_4$ ”, *Journal of Alloys and Compounds* 725 (2017) 1175-1181.
- [57] Sachin Tyagi, V. S. Pandey, Shivanshu Goel, Avesh Garg, “Synthesis and characterization of RADAR absorbing $\text{BaFe}_{12}\text{O}_{19}/\text{NiFe}_2\text{O}_4$ magnetic nanocomposite”, *Integrated Ferroelectrics* 186 (2018), 25-31
- [58] Chhavi Pahwaa, Sukhleen Bindra Narang, Puneet Sharma, “Interfacial exchange coupling driven magnetic and microwave properties of $\text{BaFe}_{12}\text{O}_{19}/\text{Ni}_{0.5}\text{Zn}_{0.5}\text{Fe}_2\text{O}_4$ nanocomposites”, *Journal of Magnetism and Magnetic Materials* 484 (2019) 61-66
- [59] Bernard Dennis Cullity, Stuart R. Stock, “Elements of X-ray Diffraction” Vol. 3. New Jersey: Prentice hall (2001).
- [60] K. W. Moon, S. G. Cho, Y. H. Choa, K. H. Kim, J. Kim, “Synthesis and magnetic properties of nano Ba-hexaferrite/NiZn ferrite composites”, *phys. stat. sol. (a)* 204 (2007) 4141–4144

[61] S. Kanagesan, M. Hashim, S. Jesurani, T. Kalaivani, I. Ismail, C. S. Ahmod, “Effect of microwave sintering on microstructural and magnetic properties of strontium hexaferrite using sol–gel technique”, *J Mater Sci: Mater Electron* 24 (2013) 3881–3884

[62] H.M. Shashanka, P.N. Anantharamaiah, P.A. Joy, “Magnetic parameters of SrFe₁₂O₁₉ sintered from a mixture of nanocrystalline and micron-sized powders”, *Ceramic International* 45 (2019) 13592-13596

Turnitin Originality Report

Processed on: 12-Jul-2019 16:22 +0530

ID: 1151257421

Word Count: 6458

Submitted: 1

Ishita sharma thesis v02 By
Ishita Sharma

1% match
(publications)

[Chhavi Pahwa, Santhoshkumar Mahadevan, Sukhleen Bindra Narano, Puneet Sharma, "Structural, magnetic and microwave properties of exchange coupled](#)

[and non-exchange coupled BaFe₁₂O₁₉/NiFe₂O₄ nanocomposites". Journal of Alloys and Compounds, 2017](#)

Similarity Index	Similarity by Source
10%	Internet Sources: 2%
	Publications: 4%
	Student Papers: 7%

Aditya

1% match (student papers from 19-Jul-2016)

[Submitted to Motilal Nehru National Institute of Technology on 2016-07-19](#)

1% match (student papers from 10-Nov-2011)

[Submitted to Higher Education Commission Pakistan on 2011-11-10](#)

1% match (student papers from 12-Jul-2018)

[Submitted to Savitribai Phule Pune University on 2018-07-12](#)

1% match (publications)

[G. Umashathy, G. Semuthuvan, L. John Berchmans, V. Sivakumar. "Structural, dielectric and AC conductivity studies of Zn substituted nickel ferrites prepared by combustion technique". Journal of Materials Science: Materials in Electronics, 2016](#)

< 1% match (student papers from 14-May-2019)

[Submitted to Universiti Putra Malaysia on 2019-05-14](#)

< 1% match (student papers from 13-Feb-2019)

[Submitted to Higher Education Commission Pakistan on 2019-02-13](#)

< 1% match (student papers from 23-Apr-2012)

[Submitted to Higher Education Commission Pakistan on 2012-04-23](#)

< 1% match (student papers from 05-Sep-2009)

[Submitted to Higher Education Commission Pakistan on 2009-09-05](#)

